

COATING PROCESS OF PHOTSENSITIVE CYLINDERS

Danmer Maza Quinones, danmerm@aluno.puc-rio.br

Márcio da Silveira Carvalho, msc@puc-rio.br

Department of Mechanical Engineering Pontifical Catholic University of Rio de Janeiro - PUC-Rio

Satish Kumar, kumar030@umn.edu

Department of Chemical Engineering/Mat Sci University of Minnesota

Abstract. Photosensitive cylinders are used in printing arts and more particularly in electrophotographic printing (xerographic copy). The photosensitive coating in liquid form is applied to the cylinder, before it is solidified. The liquid is applied to the cylinder through a needle applicator that translates along the direction of the cylinder axis. The cylinder rotates during this process in order to cover the entire surface. Therefore, the liquid is applied in a spiral pattern. To help spread the liquid over the cylinder surface and improve the thickness uniformity, each liquid stream applied from the needle passes under a flexible blade. This process leads to a coating that presents a spiral pattern on the deposited layer thickness, which can cause defects on the electrophotographic process. The complete understanding of the flow is vital to the optimization of the process. A theoretical model of the thin film flow over the surface of a rotating cylinder is presented here. It is based on the lubrication approximation considering a thin precursor film in front of the apparent contact line. The resulting non-linear fourth-order PDE for the film thickness was solved by a second-order finite difference method. The time discretization was done by the implicit Crank-Nicholson scheme. The non-linear algebraic equation at each time step was solved by Newton's method. The results show how the uniformity of the deposited layer varies with process parameters and liquid properties.

Keywords: Liquid thin film, contact line, free boundary problem, finite difference methods.

1. Introduction

Photosensitive cylinders are used in the printing art and more particularly in Electrophotographic Printing. The coating is applied to the cylinder by rotating it about its longitudinal axis and applying the liquid from an applicator in a spiral pattern as shown in Fig. 1a. This process may lead to a non-uniform thickness profile on the roll surface (see Fig. 1b) if the operating parameters are not properly chosen. As in many other coating applications, the challenge is to obtain a uniform liquid layer thickness as fast as possible. The goal of this research is to develop a theoretical model in order to better understand how the different parameters affect the uniformity of the liquid layer produced by liquid stream applied from a needle that is deposited on a rotating cylinder by the process described above. The 3-D transient liquid flow is modeled using lubrication approximation and the appropriate boundary condition at liquid-air interface. The Navier-Stokes equations are simplified into a fourth-order partial differential equation that describes how the liquid layer thickness varies with time and position.

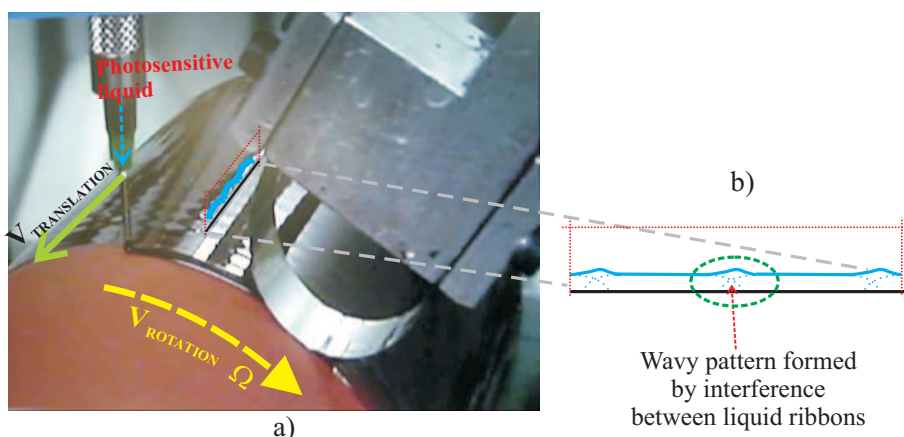


Figure 1. Coating process of photosensitive cylinder

Development of this complex theoretical model has been made by steps as shown in Fig. 2. First, the thin film flow over an inclined plane with two feed ports was analyzed, the goal was to study how two liquid streams originated from the feed ports merges and flow down the plane. The second step correspond to the two-dimensional analysis of a thin film over a rotating cylinder. The goal was to study how the viscous drag from the roll rotation, surface tension forces and

gravitational forces affect the thickness profile along the azimuthal and axial direction. The last and third step, reported here, is the combination of the two previous one, and correspond to the complete Three-dimensional thin film flow over a rotating cylinder with a moving feed port.

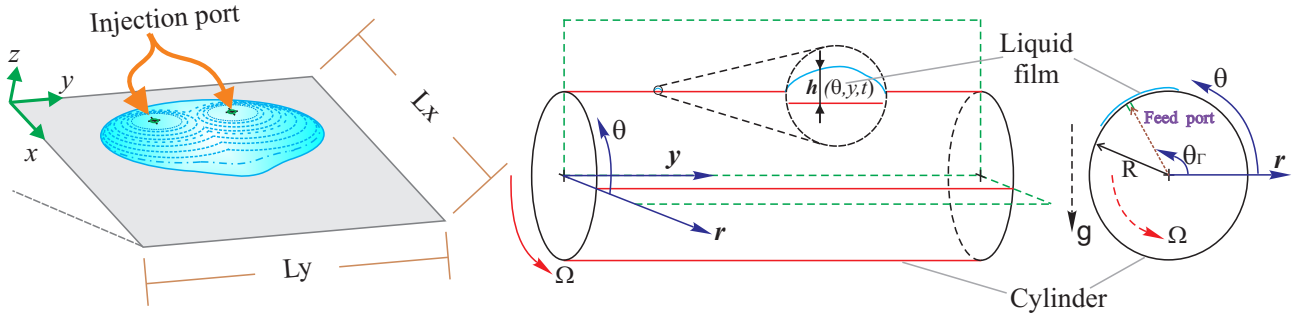


Figure 2. Sequence of modeling: over a plane and over a cylinder.

2. Three-dimensional film flow on rotating horizontal cylinder with moving feed ports

The liquid is applied to the cylinder through a needle applicator, of radius R_f , which translates along the direction of the cylinder axis at constant speed V_{need} as shown in Fig. 1a. The cylinder of radius R is rotating about its axis of revolution at constant angular speed Ω . The axis is held perpendicular to gravity g . In addition to the gravitational force, viscous and capillary forces are potentially important in this flow. The liquid is assumed to be an incompressible and Newtonian and the cylinder is assumed completely wet. It is subject to a no-slip boundary condition at the moving wall and force balance and kinematic conditions on the moving free surface.

2.1 Lubrication model

In practical coating applications, the characteristic layer thickness H is always very small, $\epsilon = H/R \ll 1$ and $Re = \rho UR/\mu \ll 1$, which allows a simplified analysis based on the lubrication theory (Panton, 1996 and Oron, 1997). With the classical simplifying assumptions of the lubrication theory, the complex 3D-Navier Stokes equation, that describes this problem, is reduced to a single non-linear fourth-order PDE describing time evolution of the free surface $h(\theta, y, t)$. Weidner et al. (1997) and Evans et al. (2005) have analyzed the coating on a stationary and rotating cylinder surface respectively. However, that coating process is different, in the present work, the coating is formed by using a moving injection port. The equation obtained by Weidner and Evans contain all the essential physics of the present problem that include "dragging" of liquid by rotation, and drainage due to the azimuthal and radial components of gravity. It is important to mention here that the fluid is assumed to be injected through a circle of radius R_f from inside to outside of cylinder (as shown in Fig. 3) centered initially around the point $(\theta_{cp}, y_{cp}(t=0))$ with a parabolic velocity profile. This approach was validated in previous steps when we analyzed the flow over an inclined plane with two feed ports.

The dimensionless evolution equation for the coating thickness, $\bar{h} = h/(\epsilon R)$, with injection port is given by:

$$(1 + \epsilon \bar{h}) \frac{\partial \bar{h}}{\partial \bar{t}} = -\epsilon \bar{\nabla} \cdot \left\{ \frac{\bar{h}^3}{3Bo} \bar{\nabla}(\bar{h} + \bar{\nabla}^2 \bar{h}) + \frac{\bar{h}^3}{3} [W^2 - \sin \theta] \bar{\nabla} \bar{h} \right\} + \frac{\partial}{\partial \theta} \left[\left(\frac{\bar{h}^3}{3} + \epsilon \frac{\bar{h}^4}{2} \right) \cos \theta \right] - \frac{MW}{\epsilon^2} \frac{\partial}{\partial \theta} \left(\bar{h} + \epsilon \frac{\bar{h}^2}{2} \right) + \frac{(1 + \epsilon \bar{h})}{\epsilon^3} M \bar{\Phi}, \quad (1)$$

where, $\bar{t} = tU/R$ with $U = \rho g H^2 / \mu$ and $\bar{\nabla} = e_\theta (\frac{\partial}{\partial \theta}) + e_y (\frac{\partial}{\partial \bar{y}})$ and $\bar{\nabla}^2 = \frac{\partial^2}{\partial \theta^2} + \frac{\partial^2}{\partial \bar{y}^2}$

The injection velocity, normal to the cylindrical surface, $\bar{\Phi}$ is defined as Schwartz and Michaelides (1988):

$$\bar{\Phi}(\theta_{cp}, \bar{y}_{cp}(t)) = \begin{cases} \frac{2\bar{\Gamma}}{\pi \bar{R}_f^2} \left[1 - \left(\frac{\bar{r}_\phi}{\bar{R}_f} \right)^2 \right] & \text{when } \bar{r}_\phi \leq \bar{R}_f; \\ 0 & \text{when } \bar{r}_\phi > \bar{R}_f. \end{cases}$$

$$\bar{r}_\phi = [(\theta - \theta_{cp})^2 + (\bar{y} - \bar{y}_{cp}(t))^2]^{\frac{1}{2}} \quad (2)$$

The position $\bar{y}_{cp}(t)$ is updated by \bar{V}_{need} at each time step Dt , and so: $\bar{y}_{cp}(t) = \bar{y}_{cp}(0) + \bar{V}_{need} \times Dt$.

We define the dimensionless viscosity $M = \mu/(\rho \sqrt{gR^3})$, dimensionless rotation rate $W = \Omega/(\sqrt{g/R})$, Bond number $Bo = (\rho g R^2)/\sigma$, dimensionless injection rate $\bar{\Gamma} = \Gamma/(\sqrt{gR}R^2)$ where Γ is the flow rate and the dimensionless

translation speed $\bar{V}_{need} = V_{need}/U$. The behavior of the coating process is determined by all those dimensionless parameters together with the initial conditions.

Due to the well-known contact line paradox (macroscopic divergence of the viscous dissipation rate), theoretical and computational methods require some regularizing mechanism. There are two different approaches in the literature. One possibility is to relax the no-slip boundary condition at fluid-solid interface, introducing a slipping length l_s . The other approach is to assume the existence of a thin precursor film H_F ahead of apparent contact line. Diez, Kondic and Bertozzi (2001), made an extensive comparison of these regularizing mechanisms. The main conclusion of these studies was that the precursor film model produced equivalent results to slip models when $H_F = l_s$. Being that the computational performance of the precursor model is much better. Wherefore is used this approach in this work.

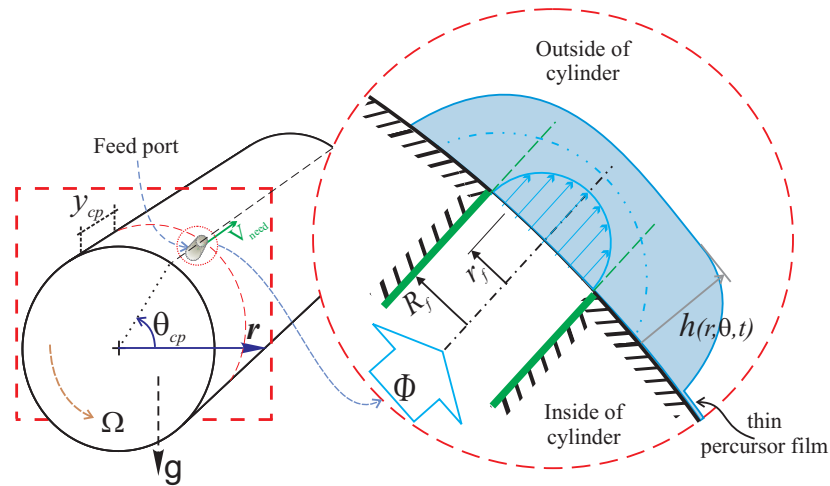


Figure 3. Sketch of injection port assumption

2.2 Numerical model

In developing a numerical model, it is convenient, though by no means essential, to have all lengths measured using a common length scale. We choose to measure all lengths, including coating thickness, in units of R , and neglecting the term $(\epsilon h) \partial h / \partial t$ of the Eq. 1 as suggest by Evans et al. (2005). With these changes and dropping bars on scaled quantities the Eq. 1 become:

$$\frac{\partial h}{\partial t} = -\nabla \cdot \left\{ \frac{h^3}{3Bo} \nabla (h + \nabla^2 h) + \frac{h^3}{3} [W^2 - \sin \theta] \nabla h \right\} + \frac{\partial}{\partial \theta} \left(\frac{h^3}{3} \cos \theta \right) - MW \frac{\partial h}{\partial \theta} + M\Phi \quad (3)$$

According to the physics of the problem, in θ direction, we need to apply a periodic boundary condition(BC), that is:

$$h(\theta + 2\pi, y, t) = h(\theta, y, t) \quad (4)$$

for all y domain. In the y direction we impose reflection symmetry boundary conditions, or zero flux, at $y = 0$ and $y = L_y$ for all θ domain. This B.C. belong to Neumann B.C., sometimes called natural boundary conditions, in which one of the derivatives is specified:

$$\frac{\partial h}{\partial y} = \frac{\partial^3 h}{\partial y^3} = 0 \quad \text{em } y = 0, \quad \text{e } y = L \quad (0 \leq \theta \leq 2\pi) \quad (5)$$

The equation 1 is a fourth-order, non-linear partial differential equation. This equation and its initial and boundary conditions were discretized using finite-difference approximations. The discretization used here is the second-order scheme proposed by Diez and Kondic (2002). Because the precursor film thickness is very small and the derivatives near the apparent contact line very high, discretization errors may lead to negative values of the film thickness. It is important to use a positive preserving scheme (PPS) in the finite difference discretization. The time discretization was done by a Crank-Nicholson scheme. The resulting non-linear set of algebraic equations was solved by the aid of Newton's method. A linear extrapolation of the two previous solution is used to calculate the initial guess and the time step is adjusted such that the number of Newton's step remains inside a given range.

3. Validation

First our numerical method was validated by comparing the predictions to two classical solutions. The first problem was solved by Moffatt (1977), and the solution represents a balance between flow due to drainage and cylinder rotation

at relatively high rotation rates. The second problem consist of flow when the cylinder is stationary and the coating configuration is unstable. This instability leads to the formation of drops at the cylinder underside, which is supported by surface tension. Here, the model was validated by comparing the prediction of Rayleigh-Taylor instabilities reported by Weidner et al. (1997).

3.1 Effect of cylinder rotation

Moffatt used kinematic wave theory and predicted a critical value of rotation speed W_c , below which there is no steady solution involving only gravity-driven drainage and fluid advection by rotation and above this rotation rate, solutions are smooth. For values of $0 < W < W_c$ a final steady state was reached. Some of these are shown here for a cylinder with radius $R = l_c$ ($Bo = 1$) where the capillary length is $l_c = \sqrt{\sigma/\rho g}$, $M = 0.007$, and starting with a layer of uniform thickness $h_0 = 0.03162R$. With these parameters, the critical speed corresponds to $W = W_c = 0.287$. Steady solutions obtained using our model with $N_\theta = 200$ and $N_y = 80$ are shown for $W = 0.01, 0.03, 0.05, 0.1, 0.15, 0.2, 0.25$ and 0.287 in Fig. 4. When the cylinder is stationary ($W = 0$) a large drop forms on the underside of the cylinder. Fluid continues to drain into this drop even at very large times. The coating layer is symmetric about a vertical axis at all times. When the cylinder is rotated, fluid is carried toward the upward-moving side of the cylinder, and vertical symmetry is lost. As W approaches W_c , the layer becomes more uniform, and the point of maximum layer thickness moves upward toward $\theta = 0$. Figure 4 shows the maximum film thickness of the final solution in (a) and the location where this occurs in (b). Increasing rotation reduces the thickness of the drop smoothly. The minimum film thickness and its location are also showed in Fig. 4. For a stationary cylinder, the minimum thickness should be zero, but this is not attained in finite time.

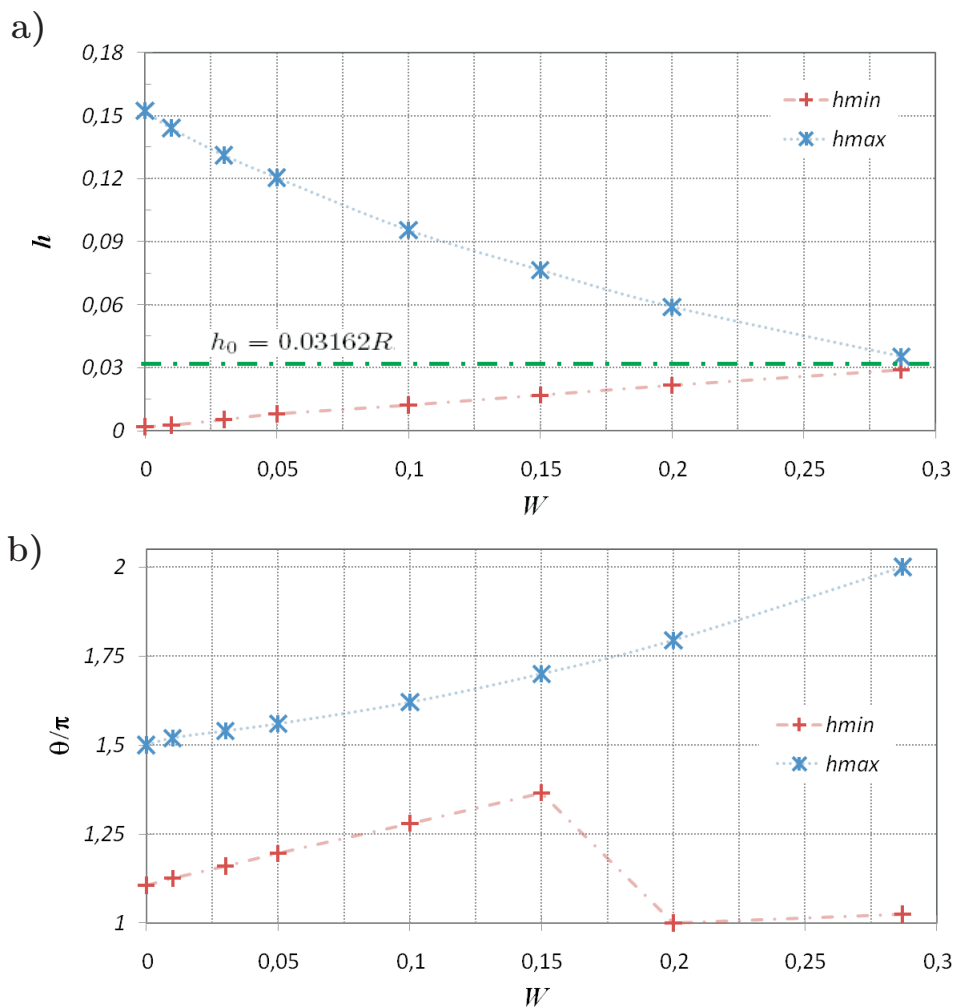


Figure 4. Extremes of coating thickness on a one-dimensional rotating cylinder, as the rotation parameter W is varied. (a) Maximum (*) and minimum (+) thickness of the steady state solution. (b) Location of the points of maximum (*) and minimum (+) thickness.

3.2 Rayleigh-Taylor instability

This instability is caused by the combined effects of surface tension and gravity when the cylinder is stationary. Gravity has a destabilizing effect on a layer of dense fluid which is above a less-dense layer. This leads to the formation of drops on the underside of a plate, which are supported by surface tension. This problem was considered in detail by Weidner et al (1997). Our model was used for a simulation of a stationary cylinder ($W = 0$) with $R = l_c$ so $Bo = 1$ and with an initial layer of thickness $h = 0.1R$, with random noise of 1% of the mean thickness in both the θ and y directions, was allowed to drain. A mesh of 40×100 grid points was used on a cylinder of length $L = 5\pi R$. The resulting coating is symmetric in a vertical plane (through $\theta = \pi/2$ and $\theta = 3\pi/2$).

Our results, with those parameters, are similar to Weidner et al results. We found the similar characteristic wavelength value for the same initial disturbance, $\lambda_{character} = 10.2$, that obtained by Weidner $\lambda_{character} = 10.5$.

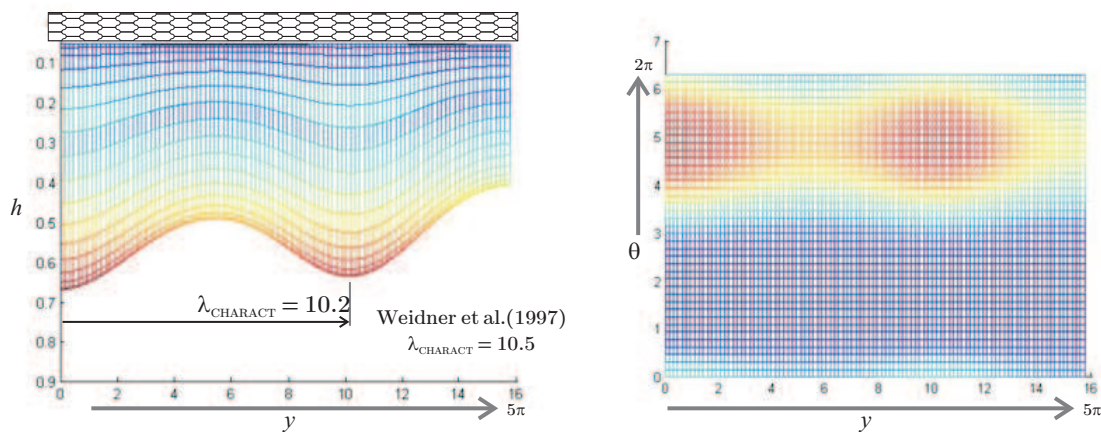


Figure 5. Film thickness at the cylinder underside, $\theta = 3\pi/2$, for a stationary cylinder. The cylinder radius $R = l_c$, was coated with a film of thickness $h=0,1$ at $t = 0$

4. Results and discussion

In choosing parameters for simulations, there are constraints on two of six dimensionless groups Bo, M, W, H_F, V_{need} and Γ . First is coating thickness that depend of Γ must be small to ensure the validity of lubrication theory. In the industry, the radius of those photosensitive cylinders are around $R = [5.08 - 10.16]cm$ exhibiting films thickness about $h = [5 - 250]\mu m$ that guarantee the application of the present model. Second one is the thin precursor film H_F , in front of the apparent contact line, which must be small to avoid results shifted in time as mentioned by Diez and Kondic (2002). This shift is due to a decreased viscous dissipation rate for larger H_F .

Here, the model is used to obtain predictions taking Γ and V_{need} in combination with the other parameters, as referred to section 2.1 We have taken into account situations when the liquid is injected through a feed port to coat the cylinder surface. Initially, advection of liquid by rotation of the cylinder was considered. Therefore, in this case $V_{need} = 0$. Then, spreading of a liquid ribbon on the top side of the cylinder was tested. The liquid ribbon was obtained considering Γ and V_{need} constant for a stationary cylinder, with $W = 0$. After that, effect of rotation rate on the coating process was tested with Γ and V_{need} constant. we show that the feed port speed needs to be adjusted depending on the rotational speed of the cylinder in order to obtain a full coverage. And finally, after choosing the appropriate values of the parameters for coating photosensitive cylinders, the leveling effect was analyzed for different liquid properties. In all these cases a thin precursor film $H_F = 3 \times 10^{-5}$ ahead of the apparent contact line was used.

4.1 Advection effect by rotation

Simulations were performed for a case when the liquid was applied from an applicator with $R_f = 0.25$, located at the fix point $(\theta_{cp}, y_{cp} = L_Y/2)$ with a injection rate $\Gamma = 0.001$ on a cylinder with radius $R = l_c$ ($Bo = 1.0$) rotating at $W = 5.0$ and $M = 0.007$ on a grid with $N_\theta = 400$ and $N_y = 100$ into a domain $L_\theta = 2\pi$ and $L_y = \pi/2$. At early times a single drop is formed. Then, it is advected by rotation bringing forth a liquid ribbon along the θ direction as showed in Fig.6a. This graphic shows the coating film in θ and y domain where the port injection was fixed at $(\theta = 135^\circ, y = L_Y/2)$ after some time, the liquid coated the entire circumference at $y = L_Y/2$. The Figure 6b show the film thickness profile along θ domain measure at $y = L_Y/2$ when liquid is applied at different port position (as showed in the Fig. 6c where (1) $(\theta = 135^\circ, y = L_Y/2)$, (2) $(\theta = 90^\circ, y = L_Y/2)$ and (3) $(\theta = 45^\circ, y = L_Y/2)$. Peaks are present in the front of

the profiles as a result of the motion due gravitational forces. This undesirable configuration may be smoothed when the position of the port injection is changed. On the first position, case (1), the component of gravity, tangent at the cylinder surface, is parallel to velocity rotation in that position. But, in case (3) those components are completely opposed between them. This position avoids drainage, of the initial drop formed at early times, due to gravity.

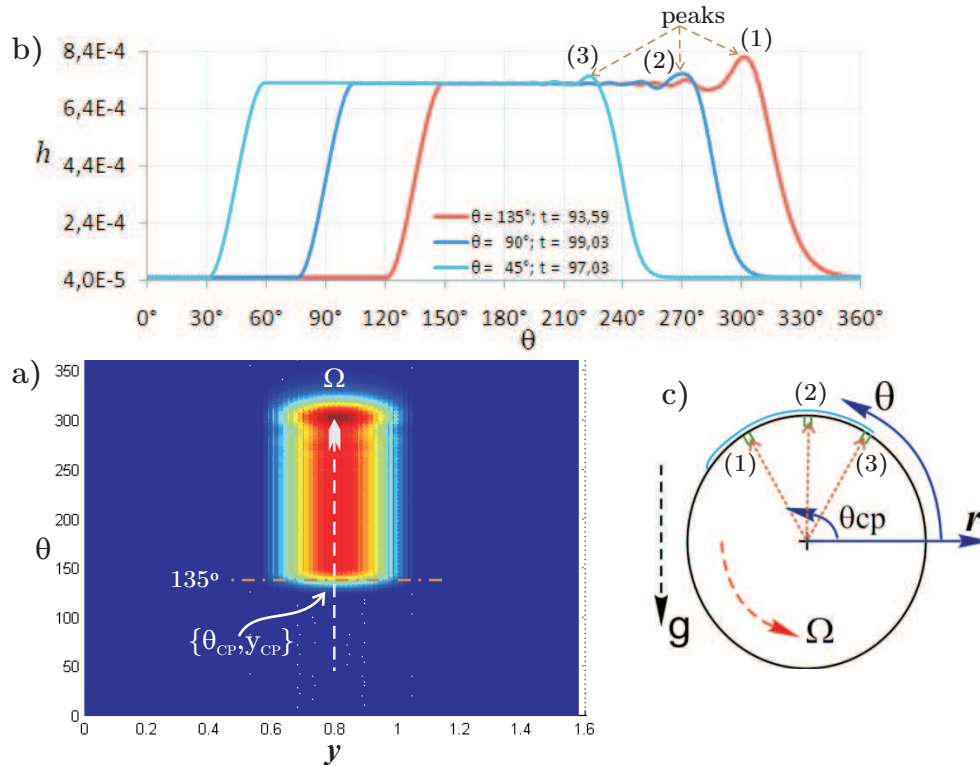


Figure 6. Rotating cylinder with injection and stationary feed port

4.2 Spreading effect over the cylinder surface

Spreading of liquid on incline plane was analyzed in previous steps where the lubrication approximation approach is applied successfully. Here, this present model is tested to know how the liquid ribbon spread along the cylindrical surface. The liquid ribbon is deposited by injection of liquid from a moving feed port with $R_f = 0.25$, at fix θ position (at top side of the cylinder), on a stationary cylinder. Figure 7b) shows the liquid ribbon obtained with $Bo = 1.0$, $M = 0.007$, $W = 0.0$, $R = lc$, $R_f = 0.25$, $H_F = 3 \times 10^{-5}$, $\Gamma = 0.001$, $V_{need} = 0.001$. In $t = 33.8$ the liquid ribbon is deposited along of y domain preestablished. Thereafter, liquid injection is stopped and then the spreading, by effect of gravitational and surface tension force, appears after some time as shown in Fig. 7a. Grid with $N_\theta = 300$ and $N_y = 100$ was used within a domain $L_\theta = 2\pi$ and $L_y = 2\pi/3$.

4.3 Effect of feed port speed

The effect of feed port speed on the coating process is presented in Fig. 8. It is clear that the feed port speed, V_{need} , needs to be related to speed rotation, W , of the cylinder in order to obtain a full coverage. Figure 8a) shows the film coating obtained at $V_{need} = 40 \times 10^{-3}$ and considering constant the others parameters: $W = 1.5$, $Bo = 1.0$, $M = 0.007$, $R = lc$, $R_f = 0.25$, $H_F = 3 \times 10^{-5}$, $\Gamma = 0.001$ and $(\theta_{cp,t} = 135^\circ, y_{cp})$. This rotation rate is not enough to cover at least part of θ domain. Decreasing the value of feed port speed to $V_{need} = 4 \times 10^{-3}$, holding others parameters at the same value, the cylinder surface is partially covered as shown in Fig. 8b following a spiral pattern. On the other hand, if V_{need} decreases more opposite situation compared to the first case is obtained (see Fig. 8c). Grid with $N_\theta = 300$ and $N_y = 150$ was used within a domain $L_\theta = 2\pi$ and $L_y = \pi$.

4.4 Effect of leveling process

We have chosen the appropriate values of those parameters that approximate the coating process of the photosensitive cylinder. The film thickness over the entire domain is show in Fig. 9. A Wavy pattern is observed as a result by the interference between liquid ribbons originated from the feed port. The dynamics of the flow can be characterized by

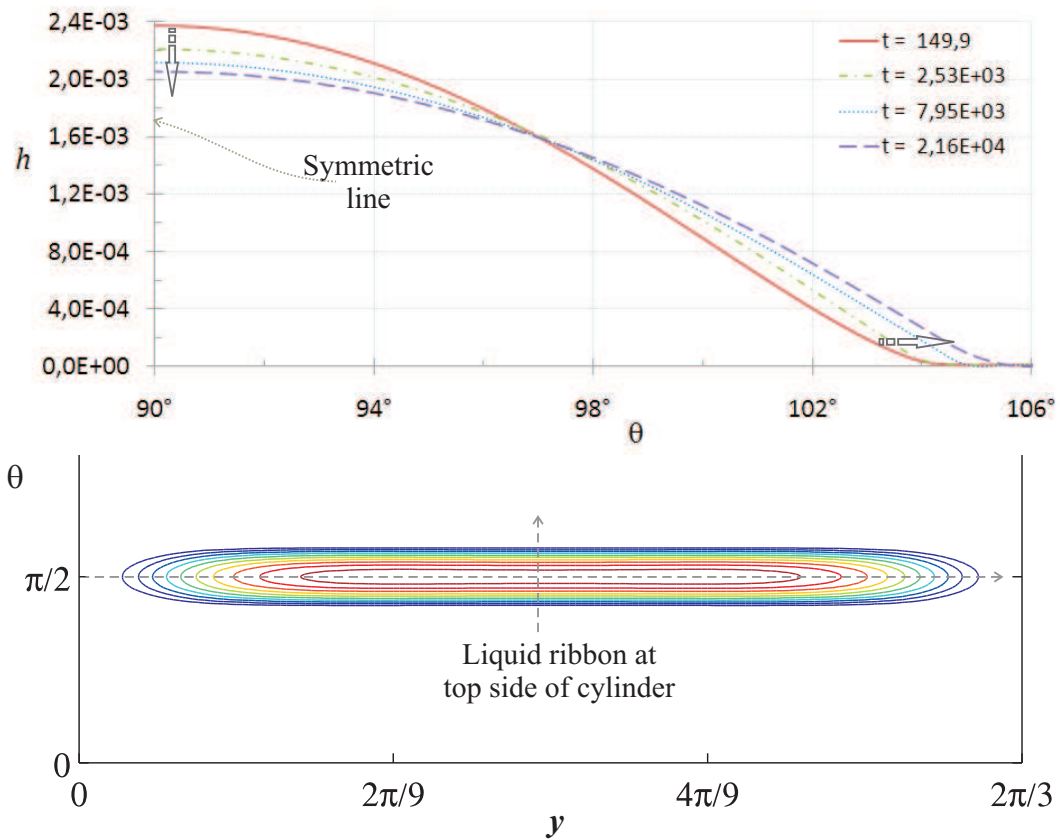


Figure 7. Spreading effect in a liquid ribbon over the cylinder surface

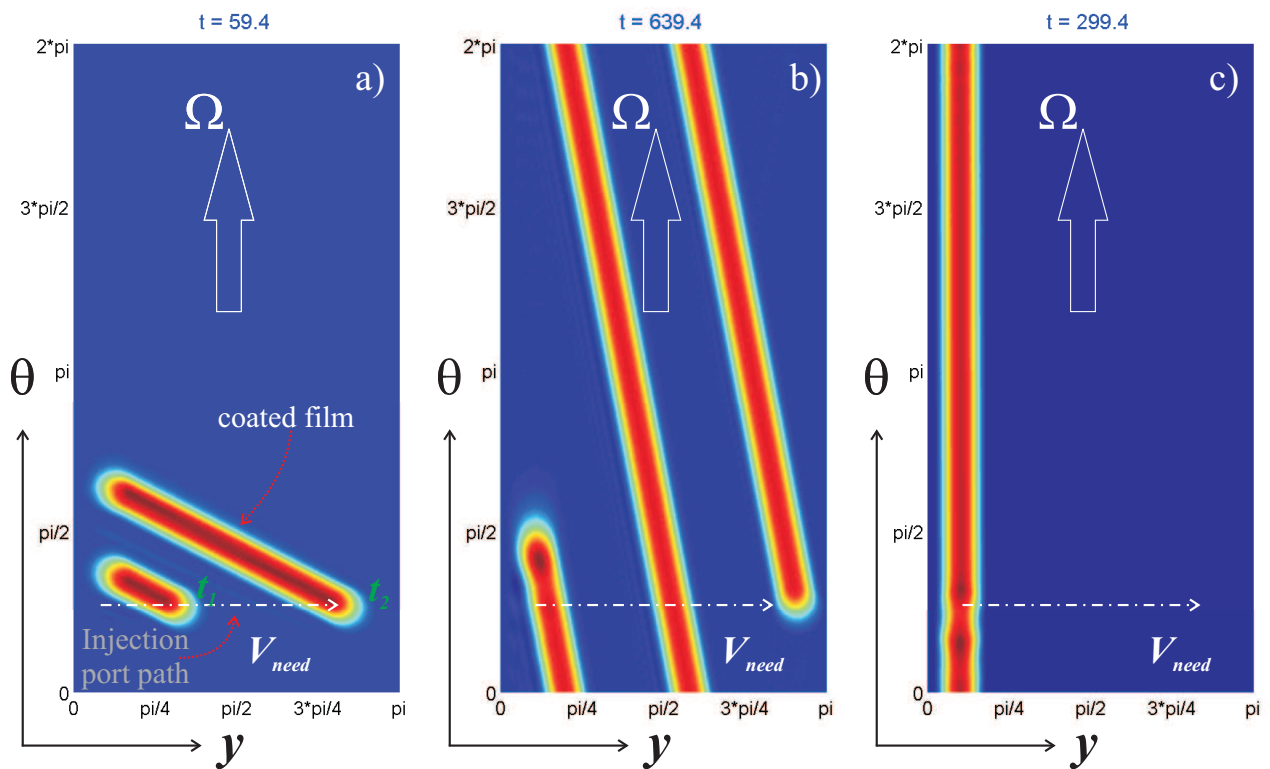


Figure 8. Effect of feed port speed: a) $V_{need} = 40 \times 10^{-3}$; b) $V_{need} = 4.0 \times 10^{-3}$ and c) $V_{need} = 0.4 \times 10^{-3}$

the parameters indicated in section 2.1 But, here we have focused just in Bo . Simulation was performed to different Bo numbers using a grid with $N_\theta = 300$ and $N_y = 100$ into a domain $L_\theta = 2\pi$ and $L_y = 2\pi/3$ and considering the others parameters as constant: $W = 1.5$, $M = 0.007$, $R_f = 0.25$, $H_F = 3 \times 10^{-5}$, $\Gamma = 0.001$, $V_{need} = 1.0e - 3$ and $(\theta_{cp,t} = \pi/2, y_{cp}) = 1.25 \times R_f$. Two stages were used to analyze the leveling effect. Plot 10a represent the first one, when the feed port reaches the end of the cylinder. This graphic represent the film thickness profile along the axial direction, y , measure at $\theta = \pi$ position for different bound numbers ($Bo = 100, 1.0, 0.1$) at $t = 1.52 \times 10^3$. For $Bo = 100$ the leveling effect is not noted and the wavy pattern remains constant. It is interesting to note that the Bond number is often large, suggesting that surface tension only makes a small contribution to the pressure. However, where large changes in h occur, the curvature is large, and surface tension is responsible for smoothing the solution. When $Bo = 0.1$ the surface tension attempt to level the wavy pattern. This effect is observed in the interval $y[0.4; 1.0]$ that correspond to the interaction of the first two deposited layer. The second stage represents the continuation of the previous one but with the stationary cylinder, $W = 0$, and $\Gamma = 0$. Figure 10b exhibits the film thickness profile at $t = 1.37 \times 10^4$ measure at the same θ position as showed in the fig. 10a. It is seen that at relative large time an amount of liquid soon accumulates at the bottom side of the cylinder. In this last figure can observe that the wavy pattern is removed for $Bo = 0.1$. Surface tension forces were strong enough to level the wavy pattern formed by coating process.

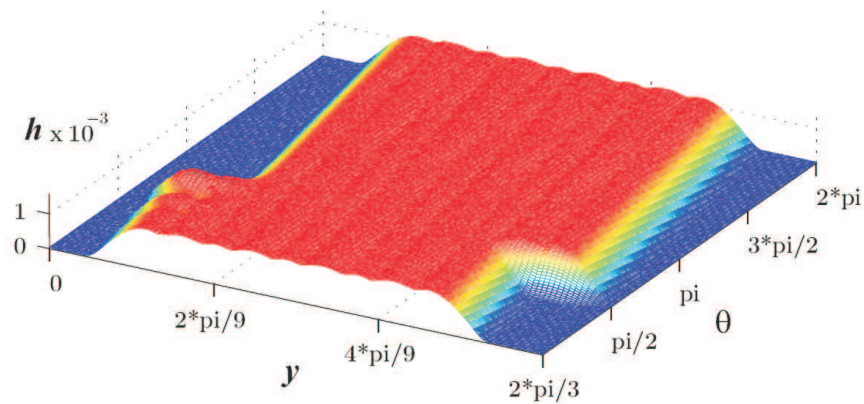


Figure 9. Coating film thickness along the θ - y domain after have chosen appropriate parameters

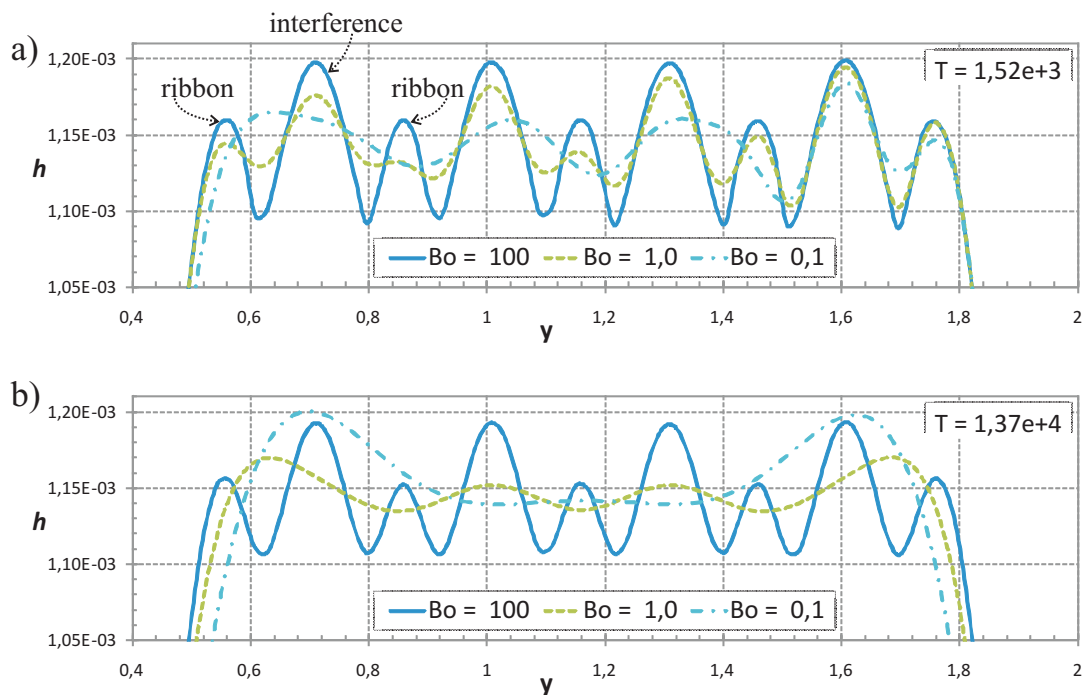


Figure 10. Effect of leveling process

5. Final remarks

We presented a model based on the thin film flow equation that is able to describe the coating process of cylinders. The results shows how the different parameters affect the uniformity of the deposited layer and can be used to optimize the process.

6. Acknowledgements

This work was funded by CNPq (Brazilian Research Council) and by Xerox Corporation through the Industrial Partnership for Research in Interfacial and Materials Engineering (IPRIME) of the University of Minnesota.

7. References

- Panton, R. L., 1996, "Incompressible Flow", Wiley Interscience Publication, USA.
- Oron, A.; Davis, S. H. and Bankoff, S. G., "Long-scale evolution of thin liquid films", *Rev. Mod. Phys.*, 138(2), pp. 449-479
- Weidner, D. E., Schwartz, L. W. and Eres, M. H., 1997, "Simulation of coating layer evolution and drop formation on horizontal cylinders" *J. Colloid Interface Sci.* 187, 243
- Evans, P. L., Schwartz, L. W. and Roy, R. V., 2005, "Three-dimensional solutions for coating flow on a rotating horizontal cylinder: Theory and experiment", *Phys. Vol.* 17, 8.
- Schwartz, L. and Michaelides, E., 1988, "Gravity flow of a viscous liquid down a slope with injection", *Letters*.
- Diez, J., Kondic, L. and Bertozzi, A. L., 2001, "Global models for moving contact lines", *Phys. Rev. E*, 63, pp. 011208/1-13
- Diez, J., Kondic, L., 2002, "Computing three-dimensional thin film flows including contact lines", *J. Comp. Phys.* 183 p.274.
- Moffatt, H. K., 1977, "Behavior of a viscous film on the outer surface of a rotating cylinder", *Journal de Mecanique*, 16(5), pp. 651-673.

8. Responsibility notice

The author(s) is (are) the only responsible for the printed material included in this paper